Tuning Diffusion and Friction in Microscopic Contacts By Mechanical Excitations

Z. Tshiprut,[1] A. E. Filippov,[2] and M. Urbakh[1]
[1]*School of Chemistry, Tel Aviv University, 69978 Tel Aviv, Israel*
[2]*Donetsk Institute for Physics and Engineering of NASU, 83144, Donetsk, Ukraine*
(Received 1 March 2005; published 29 June 2005)

We demonstrate that lateral vibrations of a substrate can dramatically increase surface diffusivity and mobility and reduce friction at the nanoscale. Dilatancy is shown to play an essential role in the dynamics of a nanometer-size tip which interacts with a vibrating surface. We find an abrupt dilatancy transition from the state with a small tip-surface separation to the state with a large separation as the vibration frequency increases. Atomic force microscopy experiments are suggested which can test the predicted effects.

DOI: 10.1103/PhysRevLett.95.016101 PACS numbers: 68.35.Af, 05.40.−a, 46.55.+d

Because of its practical importance and the relevance to basic scientific questions, there has been a major increase in the activity in studies of dynamics in nanoscale confinement during the last decade [1–4]. Substantial progress in understanding the leading factors that determine the dynamics in confining systems has opened new possibilities to modify and control motion at the nanoscale [5–15]. The difficulties in realizing an efficient control of motion are related to the complexity of the task, namely, dealing with systems with many degrees of freedom under a strict size confinement, which leaves very limited access to interfere with the system in order to be able to control.

In this Letter we investigate the effect of lateral vibrations of a substrate on diffusivity, mobility, and friction at the nanoscale. We demonstrate that manipulations by mechanical excitations when applied at the right frequency and amplitude can dramatically increase surface diffusion and mobility, and reduce friction. The proposed approach differs from earlier suggestions of controlling friction via normal vibrations [8–11,13]. The predicted effects should be amenable to atomic force microscopy (AFM) tests using, for instance, shear modulation mode [14,16] or applying ultrasound to the sample [17,18]. The model can also be used in studies of contact mechanics of a probe interacting with oscillating quartz crystal microbalance surfaces which provide unique information on interfacial properties under high-frequency shear [19–21].

In order to study the effect of lateral vibrations on diffusion and friction in the context of AFM, we introduce a model of a tip interacting with a substrate, which oscillates in the lateral direction. The motion of the tip in the lateral, and normal, directions is governed by the coupled Langevin equations:

$$M\ddot{x}(t) = -\eta_x(z)[\dot{x}(t) - \dot{x}_0(t)] - \partial U(x - x_0, z)/\partial x + F_x + f_x \qquad (1)$$

and

$$M\ddot{z}(t) = -\eta_z(z)\dot{z}(t) - \partial U(x - x_0, z)/\partial z + F_z + f_z \qquad (2)$$

where

$$U(x - x_0) = U_0\left[1 + \sigma \sin\left(\frac{2\pi}{b}(x - x_0)\right)\right]\exp(1 - z/\lambda),$$
$$\eta_{x,z}(z) = \eta^0_{x,z}\exp(1 - z/\lambda). \qquad (3)$$

Here M and x, and z are the mass, the lateral, and the normal coordinates of the tip, $U(x, z)$ is the potential experienced by the tip due to the interaction with the substrate, b is its periodicity in the lateral direction, and σ characterizes the amplitude of corrugation in the x direction. The parameters η_x and η_z are responsible for the dissipation of the tip kinetic energy due to the motion in the x and z directions, respectively. These terms account for the dissipation due to phonons and/or other excitations [3,15]. Here we take into account the dependence of U and $\eta_{x,z}$ on the tip-substrate separation [11]. As an example, we assume an exponential decrease of U and $\eta_{x,z}$ with a rate λ^{-1} as z increases. The tip is held at the surface by a normal load $F_z = K_z[z_0 - z(t)]$ applied by a linear spring of spring constant K_z. In friction experiments the tip is laterally pulled, $F_x = K_x[vt - x(t)]$, by a spring of spring constant K_x connected to a stage which moves with a constant velocity v. The effect of lateral vibrations of the substrate is included through a time dependence of its position, $x_0 = A_0 \sin(2\pi\omega t)$, where A_0 and ω are the amplitude and the frequency of the oscillations. The random forces, $f_{x,z}$, represent thermal noise satisfying the fluctuation-dissipation relation, $\langle f_i(t)f_j(0)\rangle = 2\eta_i k_b T\delta(t)\delta_{i,j}$, where $i, j = x, z$.

It is convenient to introduce the dimensionless coordinates and time $X = x/b$, $Z = z/b$, $\tau = t\omega_0$, where $\omega_0 = (1/b)\sqrt{U_0\sigma/M}$ is the frequency of the small oscillations of the tip in the periodic potential. The dynamical behavior of the system is determined by the following dimensionless parameters: $A = A_0/b$, $\Omega = \omega/\omega_0$, k_BT/U_0, $\eta_{x,z}/M\omega_0$, λ/b, $K_xb^2/(4\pi^2U_0\sigma)$, $K_z\lambda^2/U_0$, and $\tilde{v} = v/(\omega_0 b)$.

First, we consider the effect of the substrate vibrations on surface diffusion, which occurs in the absence of the lateral driving force, $F_x = 0$. We start from the case of one-dimensional motion of the tip, which takes place for a stiff normal spring, $K_z \gg U_0(1+\sigma)/\lambda^2$. Then the distance between the tip and the surface is constant, $z = z_0$. Equation (1) shows that the substrate vibrations cause a time-periodic (ac) force acting on the tip, $F_{\rm ac} = M(2\pi\omega)^2 A_0 \sin(2\pi\omega t)$. This force presents the effect of inertia. Its amplitude depends on both the amplitude and frequency of vibrations. Recent studies of surface diffusion under ac forcing [6,7] demonstrated that the diffusivity D may be strongly enhanced and even exceed the free (Brownian) diffusivity, $D_{\rm free} = k_B T/\eta_x$, for an optimal matching of the driving frequency, ω, and the amplitude A_0. A similar effect has been found in our calculations. As an example, we show in Fig. 1 the frequency dependence of the diffusion coefficient, $D(\Omega)$, calculated for two vibration amplitudes, $A = 1$, 2. For both amplitudes the diffusion coefficient exhibits a resonance behavior for frequencies, which are close to the characteristic frequency, $\Omega = 1$. For low frequencies, $\Omega \ll 1$, the tip follows the motion of the plate, performing small oscillations around the potential minima. The energy of thermal fluctuations is essentially smaller than the height of the potential barrier and as a result, the probability to escape from the potential well is exponentially small in this case. With an increase in Ω, the tip has no time to respond to the substrate vibrations, and the amplitude of the tip oscillations increases. At resonance frequencies, $\Omega = \Omega_*$, which correspond to the maxima of the diffusion coefficient, the tip approaches the top of the surface potential at the end of half cycle of the plate vibrations, where the driving force, $F_{\rm ac} = 0$. Then, even a weak thermal noise splits the ensemble of tips into two parts that relax to the neighboring minima of the surface potential, and the resonance enhancement of diffusion is observed. A further increase of the frequency leads again to localized oscillations of the tip; in contrast to the case of low frequencies here the tip overcomes the potential barriers and oscillates between neighboring minima of the surface potential.

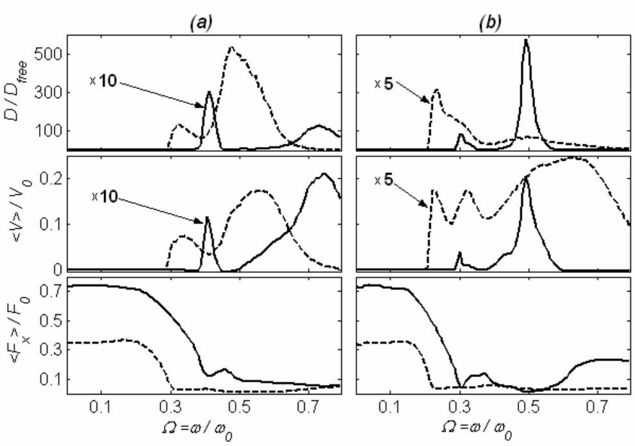

FIG. 1. Frequency dependence of the relative diffusion coefficient (top panel, $F_x \equiv 0$), the time-averaged tip velocity (middle panel, $F_x = F_{\rm dc} = 0.01 F_0$) and the friction force [bottom panel, $F_x = K_x(vt - x)$] calculated for a fixed tip-surface separation (solid curves) and including the normal motion (dashed curves); (a) $A = 1$ and (b) $A = 2$. Parameter values: $\lambda/b = 1$, $\sigma = 1$, $\eta_{x,z}/M\omega_0 = 3.2$, $k_B T/U_0 = 0.01$, $K_x b^2/(4\pi^2 U_0 \sigma) = 3.2\times 10^{-3}$, $K_z \lambda^2/U_0 = 0.63$, $F_{\rm dc}/F_0 = 0.01$, $v/V_0 = 0.16$, where $F_0 = 2\pi U_0/b$ and $V_0 = \omega_0 b$.

Our calculations suggest that the vibration-induced enhancement of the diffusion can be observed in AFM experiments. In this configuration the tip experiences the influence of two potentials: the periodic surface potential and the harmonic potential, $K_x(x - x_{\rm sup})^2/2$, due to the elastic coupling to the support of the microscope of coordinate $x_{\rm sup}$, which remains fixed. Our simulations in Fig. 2 demonstrate that the experimentally measurable root mean square displacement (rmsd) of the tip, $\Delta L(\Omega)$, exhibits a resonance enhancement for the frequency Ω_* corresponding to the maximum of the diffusion coefficient. The results for $\Delta L(\Omega)$ can be fit by the Ornstein–Uhlenbeck (OU) equation

$$\Delta L_{\rm OU} = \sqrt{D_{\rm free}\eta_x/K_x} \tag{4}$$

for the rmsd due to diffusion in the harmonic potential [22], when a free diffusion coefficient, $D_{\rm free}$, is substituted by the Ω dependent enhanced diffusion coefficient, $D(\Omega)$ (the dashed curve in Fig. 2).

Under the conditions which are typical for AFM measurements [14], $m = 8.7\times 10^{-12}$ kg, $U_0 = 0.25$ eV, and $b = 0.4$ nm, we arrive at the resonance frequency $\omega_* = \omega_0\Omega_* = 7\times 10^4$ Hz. This value lies within the frequency interval exploited by the shear modulation technique [16] and agrees qualitatively with the value of the frequency for which the resonance reduction of friction under the oscillatory drive has been observed [14]. The experiment suggested here can be considered as a diffusion

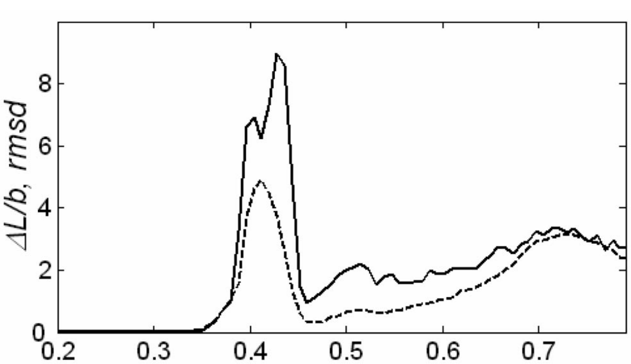

FIG. 2. Frequency dependence of the rmsd of the tip. Solid curve—numerical simulations, dashed curve—calculation according to the equation $\Delta L(\Omega) = \sqrt{D(\Omega)\eta_x/K_x}$. Parameter values: $A = 1$, $K_x b^2/[(2\pi)^2 U_0 \sigma] = 3.2\times 10^{-4}$, $K_z \to \infty$, other parameters as in Fig. 1.

"spectroscopy" of surfaces. Measuring the "spectrum" of diffusion, $D(\Omega)$, one can determine the parameters of the surface potential.

In AFM experiments the tip is held near the surface by the normal load applied through the spring with the spring constant K_z. As a result, the tip driven in a lateral direction, also performs oscillations in the normal direction [11]. The amplitude of these oscillations depends on the surface potential and the stiffness of the normal spring. The effect of normal oscillations of the tip on the lateral diffusion is clearly seen in Fig. 1 where we present a comparison between the Ω dependencies of the diffusion coefficients calculated for a fixed tip-surface separation and including the normal motion. In the latter case we also observed a giant enhancement of diffusion induced by the lateral vibrations, but the shape of $D(\Omega)$ is very different from that obtained for the one-dimensional case. In order to gain insight into the effect of normal-lateral coupling on the surface diffusion we show in Fig. 3 the frequency dependence of the time-averaged distance between the tip and the surface. This figure, as well as the tip trajectories, demonstrate the existence of two stable surface separations z_0 and z_h, which correspond to small tip oscillations in the vicinity of the potential minima (low Ω) and to the large-scale tip displacements (high Ω), respectively. The excitation of normal motion by the lateral drive becomes efficient only when the amplitude of the lateral tip oscillations is large enough to feel a nonlinearity of the tip-surface interaction. As a result, for a given driving amplitude, the dilatancy is observed only for frequencies which exceed some threshold value Ω_{th}, which depends on the potential and normal load.

Figure 3 shows a sharp transition from the state with a small tip-surface separation to the state with a large separation which occurs with increasing frequency. It must be noted that both the dilatancy transition and enhancement of diffusion originate from the excitation of the large-scale tip oscillations by the substrate vibrations. As a result, both effects arise at the same threshold frequency, Ω_{th}. However, in contrast to the dilation which takes place for all $\Omega > \Omega_{\text{th}}$, the significant enhancement of diffusion occurs only in a vicinity of the resonance frequencies for which the amplitude of tip oscillations equals to $b(1/2 + n)$, $n = 1, 2, \ldots$.

The dilatancy leads to a reduction of the amplitude of the potential corrugation and of the dissipation parameter η_x experienced by the tip. This results in a decrease of the driving frequencies and amplitudes, which correspond to the resonances of $D(\Omega)$, and to a broadening of the resonance peaks compared to the case of the constant tip-surface separation.

Substrate vibrations also cause a resonance enhancement of surface mobility which arises under the action of a time-independent (dc) force, $F_x \equiv F_{\text{dc}}$ (see Fig. 1, middle panel). It should be emphasized that in the absence of vibrations the directed motion is not detectable at the time scale of our simulations for the value of the force, $F_{\text{dc}} = 10^{-2} F_0(|F_0| = \max|\partial U/\partial x| = 2\pi\sigma U_0/b)$, chosen here.

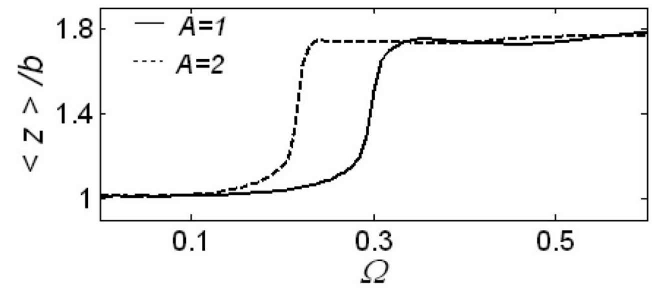

FIG. 3. Frequency dependence of the time-averaged tip-surface separation; solid curve—$A = 1$, dashed curve—$A = 2$. Parameters' values as in Fig. 1.

There is a clear correlation between the enhancement of diffusion and time-averaged tip velocity, $\langle V\rangle$ (see Fig. 1). In the case of regular diffusion caused by the equilibrium thermal fluctuations, the fluctuation-dissipation theorem suggests that there is a linear relation between the diffusion coefficient and the average velocity calculated in the limit of zero dc driving, $D = k_B T(d\langle V\rangle/dF_{\text{dc}})|_{F_{\text{dc}}=0}$. The reason why we do not observe the proportionality relation here is that the enhanced diffusion is induced by the *nonequilibrium* vibrations, and the fluctuation-dissipation theorem breaks down in this case. It should be also noted that the calculations have been done for a small but finite driving force, that can also violate the proportionality between D and $\langle V\rangle$.

The calculations performed for a dc driving force can simulate the AFM frictional response in the limit of a very weak lateral spring, $K_x \to 0$, where the applied force $F_x = K_x(vt - x)$ remains almost constant. However, for low driving velocities where a stick-slip motion is usually observed [14,15], a time variation of F_x should be taken into account. Below we focus on the effect of lateral vibrations on this regime of motion.

Figs. 1 (bottom panel) and 4 show the Ω dependence of the time-averaged friction force $\langle F_x\rangle$ and the instantaneous friction force $F_x = K_x(vt - x)$, tip displacement and tip-surface separation, respectively. One can see that, for low frequencies the lateral vibrations do not affect the frictional response. Both the spring force and displacement traces show the patterns that are typical for the stick-slip behavior, and the average force is independent of Ω. For a finite stiffness of the normal spring the tip-surface separation, which is initially z_0, at equilibrium, starts growing before a slippage occurs and stabilizes at a larger distance, z_h, as long as the motion continues (see Fig. 4). Since the static friction is determined by the amplitude of the potential corrugation, it is obvious that the dilatancy leads to a decrease of the static friction compared to the case of a constant tip-surface distance (see Fig. 1, bottom panel).

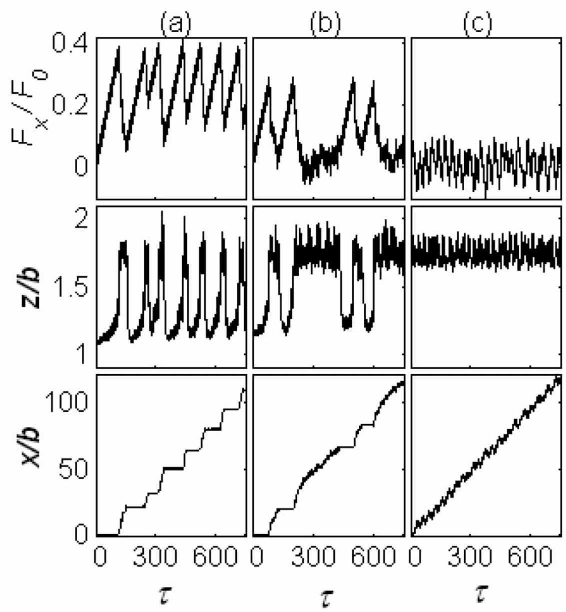

FIG. 4. Time dependencies of the relative friction force, F_x/F_0, the tip-surface separation, z/b, and the lateral displacement of the tip, x/b calculated for $A = 1$ and three frequencies: $\Omega = 0.26$ (a), 0.29 (b), and 0.32 (c). Parameters value as in Fig. 1.

In the vicinity of the threshold frequency Ω_{th} for which the enhanced diffusion is beginning to emerge, we find a drastic decrease of the kinetic friction. Figs. 1 and 4 demonstrate that the lateral vibrations not only reduce the friction force but they also transform the stick-slip motion to a ''smooth'' sliding. However, the application of lateral vibrations does not allow the complete elimination of the force fluctuations. Even under the optimal conditions the variance of the friction force remains of the order of K_xA. The transition in the lateral response is accompanied by a dilatancy transition (see the middle panel of Fig. 4).

The main feature in Fig. 1 (bottom panel) is a reduction of friction for all frequencies above the threshold one, Ω_{th}. In contrast to the enhancement of diffusion and mobility, the reduction of friction does not exhibit pronounced resonance features. This is a consequence of the fluctuations of the applied force. Contrary to the calculations of mobility, which have been done for a small constant force, in the configuration corresponding to the friction experiments the fluctuations of the applied force are of the order of K_xA, and they can be essentially larger than the average value of the force. For $\Omega > \Omega_{th}$ where the substrate vibrations induce large-scale oscillations of the tip, these fluctuations are sufficient to cause a slow motion of the tip.

In summary, we have demonstrated that lateral vibrations of the substrate can dramatically increase surface diffusivity and mobility and reduce friction at the nanoscale. We have found a sharp transition from the state with a small tip-surface separation to the state with a large separation as the vibration frequency increases.

The authors are grateful to Joseph Klafter for fruitful discussions. This work was supported by the Deutsche Forschungsgemeinschaft (HA 1517/26-1). A. E. F. thanks the ESF ''Nanotribology'' Program for financial support.

[1] R. Metzler and J. Klafter, J. Phys. A: Math. Gen. **37**, R161 (2004).
[2] *Dynamics in Small Confining Systems VI*, edited by J. T. Fourkas, P. E. Levitz, M. Urbakh, and K. J. Wahl (Material Research Society, Pittsburgh, 2003).
[3] B. N. J. Persson, *Sliding Friction, Physical Properties and Applications* (Springer, Berlin, 2000).
[4] M. Urbakh *et al.*, Nature (London) **430**, 525 (2004).
[5] R. D. Astumian and P. Hanggi, Phys. Today **55**, No. 11, 33 (2002).
[6] Hu. Gang, A. Daffertshofer, and H. Haken, Phys. Rev. Lett. **76**, 4874 (1996).
[7] M. Schreier, P. Reimann, P. Hanggi, and E. Pollak, Europhys. Lett. **44**, 416 (1998).
[8] M. G. Rozman, M. Urbakh, and J. Klafter, Phys. Rev. E **57**, 7340 (1998).
[9] J. P. Gao, W. D. Luedtke, and U. Landman, J. Phys. Chem. B **102**, 5033 (1998).
[10] M. Heuberger, C. Drummond, and J. N. Israelachvili, J. Phys. Chem. B **102**, 5038 (1998).
[11] V. Zaloj, M. Urbakh, and J. Klafter, Phys. Rev. Lett. **82**, 4823 (1999).
[12] Y. Braiman, J. Barhen, and V. Protopopescu, Phys. Rev. Lett. **90**, 094301 (2003).
[13] A. Cochard, L. Bureau, and T. Baumberger, Trans. Am. Soc. Mech. Eng. **70**, 220 (2003).
[14] E. Riedo *et al.*, Phys. Rev. Lett. **91**, 084502 (2003).
[15] M. H. Muser, M. Urbakh, and M. O.Robbins, Adv. Chem. Phys. **126**, 187 (2003).
[16] S. Ge *et al.*, Phys. Rev. Lett. **85**, 2340 (2000).
[17] F. Dinneli *et al.*, Appl. Phys. Lett. **71**, 1177 (1997).
[18] T. Hesjedal and G. Behme, IEEE Trans. Ultrason. Ferroelectr. Freq. Control **49**, 356 (2002).
[19] B. Borovsky *et al.*, J. Appl. Phys. **90**, 6391 (2001).
[20] S. Berg and D. Johannsmann, Phys. Rev. Lett. **91**, 145505 (2003).
[21] J. F. Lubben and D. Johannsmann, Langmuir **20**, 3698 (2004).
[22] H. Risken, *The Fokker-Planck Equation* (Springer, Berlin, 1996).